Trigonal Band Structure and Time-Reversal Invariance in Graphene

R. Winkler[1, 2, 3] and U. Zülicke[1, 4]

[1] *Institute of Fundamental Sciences and MacDiarmid Institute for Advanced Materials and Nanotechnology, Massey University (Manawatu Campus), Private Bag 11 222, Palmerston North, New Zealand*
[2] *Argonne National Laboratory, Argonne, IL 60439*
[3] *Department of Physics, Northern Illinois University, DeKalb, IL 60115*
[4] *Centre for Theoretical Chemistry and Physics, Massey University (Albany Campus), Private Bag 102904, North Shore MSC, Auckland 0745, New Zealand*

(Dated: January 9, 2009)

We present a symmetry analysis of the trigonal band structure in graphene. While the energy spectrum near the Fermi edge equals the spectrum of massless Dirac fermions, the transformational properties of the underlying basis functions are qualitatively different. Using group theory we develop an invariant expansion of the Hamiltonian for the electron states near the **K** points of the graphene Brillouin zone. We find that the k-linear dispersion near the band edge arises as an unusual consequence of time-reversal invariance. We suggest to divide the electronic properties of graphene into two categories, those that depend and those that do not depend on the transformational properties of the Bloch functions at **K**.

In recent years, tremendous interest has been focused on studying single layers of graphene, following the first experimental realization of this material [1]. To a large extent, these continuing efforts are motivated by the unique band structure of graphene in the vicinity of the Fermi edge. In most semiconductors, the band edges are characterized by a quadratic dispersion, with k-linear corrections possible only in inversion-asymmetric materials due to spin-orbit coupling [2]. In contrast, for graphene, the dispersion $E(\mathbf{k})$ of the uppermost valence band and the lowest conduction band is *dominated* by k-linear terms [3], $E(\mathbf{k}) \approx \hbar v k$ with Fermi velocity v. These bands touch at the points **K** and $\mathbf{K}'$ at the edge of the Brillouin zone [Fig. 1(b)] so that the resulting energy surfaces resemble those of free massless fermions described by the Dirac equation [Fig. 1(c)]. The apparent analogies between a solid-state system and relativistic quantum mechanics have greatly stimulated the interest in graphene [1, 4]. For example, it was argued that the chiral electrons in graphene can show both weak localization and antilocalization (Ref. [5] and references therein).

The group-theoretical analysis presented here shows that, nonetheless, there are important differences between electrons in graphene and massless Dirac fermions. Even though both systems can be described by the same Hamiltonian (giving also the same spectrum), the transformational properties of the underlying basis functions are qualitatively different. We suggest to divide the electronic properties of graphene into two categories, those that emerge from the linear dispersion but that are independent of the transformational properties of the basis functions and those that do reflect these transformational properties.

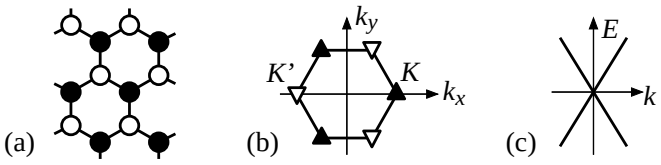

FIG. 1: (a) Honeycomb lattice of graphene. Atoms in sublattice A (B) are marked with open (closed) circles. (b) Brillouin zone and its two inequivalent corner points **K** and $\mathbf{K}'$. The remaining corners are related with **K** or $\mathbf{K}'$ by reciprocal lattice vectors. (c) Dispersion $E(k)$ near the **K** point.

The starting point of our analysis are the Bloch functions at **K** and $\mathbf{K}'$. In the commonly used tight-binding (TB) model of Refs. [3, 6] for the bonding and antibonding π bands in graphene, each of the Bloch functions can be chosen to be nonzero only on sublattice $s = A$ or B [Fig. 1(a)], i.e.,

$$\Psi_{\mathbf{K},s}(\mathbf{r}) = \frac{1}{\sqrt{N}} \sum_{\mathbf{R}_s} e^{i\mathbf{K}\cdot\mathbf{R}_s}\, \phi_\pi(\mathbf{r} - \mathbf{R}_s)\,. \qquad (1)$$

Here $\phi_\pi(\mathbf{r})$ denotes the carbon π orbital and the sum runs over the atomic positions $\mathbf{R}_s$ in sublattice s. The group of the wave vector **K** is isomorphic to the trigonal point group D_{3h} (while the point group of the honeycomb structure is D_{6h}). Projection of $\Psi_{\mathbf{K},s}(\mathbf{r})$ on the irreducible representations (IRs) of D_{3h} shows [2, 7] that these functions transform according to the two-dimensional IR Γ_6 [8, 9]. More specifically, under the symmetry operations of D_{3h}, the Bloch function $\Psi_{\mathbf{K},A(B)}(\mathbf{r})$ transforms like $|\rho_{-(+)}\rangle$, where $|\rho_\pm\rangle \equiv \frac{1}{\sqrt{2}}|x \pm iy\rangle$. Thus, from a symmetry point of view, we may identify $\{\Psi_{\mathbf{K},s}(\mathbf{r})\}$ with $\{|\rho_\mp\rangle\}$. Note that $\Psi_{\mathbf{K}',s} = \Psi^*_{\mathbf{K},s}$ [i.e., the existence of two inequivalent valleys **K** and $\mathbf{K}'$ does not cause extra degeneracies, see Eq. (5) below]. The role of $|\rho_\pm\rangle$ is thus reversed at the $\mathbf{K}'$ point: $|\rho_-\rangle$ ($|\rho_+\rangle$) corresponds to sublattice B (A).

The TB model of Refs. [3, 6] neglects the spin degree of freedom. Thus we have obtained an ordinary IR (Γ_6 of D_{3h}), which differs qualitatively from the double-group

(spinor) IRs characterizing a particle with a *genuine* spin-1/2 degree of freedom coupled to a particle's orbital motion. The double group G_d corresponding to a group G can be written as $G_d = G \oplus \bar{E}G$, where $\bar{E}$ is a rotation by 2π around an arbitrary axis. The presence of $\bar{E}$ in G_d reflects the well-known fact that spin-1/2 spinors (which may be used [8] as basis functions for the spinor IR Γ_7 of D_{3h}) change sign when rotated by 2π. The basis functions of Γ_6 do not change sign when rotated by 2π, i.e., $\bar{E}$ acts like the neutral element E. Furthermore, the point group D_{3h} contains three "vertical" reflection planes σ_v as symmetry elements [8]. Unlike spin-1/2 spinors, the basis functions of Γ_6 change sign under these reflections.

To proceed, we use the theory of invariants [2] to construct an invariant expansion for the effective Hamiltonian $\mathcal{H}(\boldsymbol{\mathcal{K}})$ describing the electron states in the vicinity of $\mathbf{K}$ and $\mathbf{K}'$. Here $\boldsymbol{\mathcal{K}}$ represents a general tensor operator, which can depend, e.g., on the components of the kinetic wave vector $\mathbf{k}$ and external electric and magnetic fields $\boldsymbol{\mathcal{E}}$ and $\mathbf{B}$. $\boldsymbol{\mathcal{K}}$ can be decomposed into irreducible tensor operators $\boldsymbol{\mathcal{K}}^{(\kappa,\lambda)}$ that transform according to the IRs Γ_κ of D_{3h}. Using the coordinate system in Fig. 1(b), we get the lowest-order tensor operators $\boldsymbol{\mathcal{K}}^{(\kappa,\lambda)}$ in Table I. Furthermore, $\mathcal{H}(\boldsymbol{\mathcal{K}})$ can be decomposed into blocks $\mathcal{H}_{\alpha\beta}(\boldsymbol{\mathcal{K}})$, where α and β denote the spaces of the n_α- and n_β-fold degenerate band-edge Bloch functions, which transform according to the IRs Γ_α and Γ_β of D_{3h}. (Without spin, we have only one band Γ_6. Below, we also derive the multiband Hamiltonian that takes into account spin.) For each block $\mathcal{H}_{\alpha\beta}(\boldsymbol{\mathcal{K}})$, one can find a complete set of linearly independent $n_\alpha \times n_\beta$-dimensional matrices $X_l^{(\kappa)}$ that transform according to the IRs Γ_κ (of dimension L_κ) contained in the product representation $\Gamma_\alpha \times \Gamma_\beta^*$. Choosing basis functions for Γ_6 that transform like $\{|\rho_-\rangle, |\rho_+\rangle\}$ we obtain the basis matrices listed in Table II. Then each block $\mathcal{H}_{\alpha\beta}(\boldsymbol{\mathcal{K}})$ can be written as

$$\mathcal{H}_{\alpha\beta}(\boldsymbol{\mathcal{K}}) = \sum_{\kappa,\,\lambda} a_{\kappa\lambda}^{\alpha\beta} \sum_{l=1}^{L_\kappa} X_l^{(\kappa)} \mathcal{K}_l^{(\kappa,\lambda)\,*}\,, \qquad (2)$$

with material-specific coefficients $a_{\kappa\lambda}^{\alpha\beta}$. By construction, each block $\mathcal{H}_{\alpha\beta}(\boldsymbol{\mathcal{K}})$ is invariant under the symmetry operations in D_{3h}. Explicitly we get up to second order in $\mathbf{k}$ (for $B = \mathcal{E} = 0$) [10, 11, 12]

$$\begin{aligned}\mathcal{H}_{66}^k \;=\; & a_{10}^{66}\mathbb{1} + a_{61}^{66}(k_x\sigma_x + k_y\sigma_y) + a_{12}^{66}(k_x^2 + k_y^2)\mathbb{1} \\ & + a_{62}^{66}[(k_y^2 - k_x^2)\sigma_x + 2k_xk_y\sigma_y] + \mathcal{O}(k^3)\,. \qquad (3)\end{aligned}$$

Third-order terms can be read off from Tables I and II. Terms of yet higher orders are constructed in a similar way. Equation (3) applies to $\mathbf{K}$. To describe $\mathbf{K}'$ within the same coordinate system, we need to substitute $(\sigma_x, \sigma_y, \sigma_z) \to (\sigma_x, -\sigma_y, -\sigma_z)$ (throughout Table II). $\mathcal{H}_{66}^k$ gives rise to a dispersion

$$E_\pm(\mathbf{k}) = a_{10}^{66} \pm a_{61}^{66}k + a_{12}^{66}k^2 \pm a_{62}^{66}k_x(k_x^2 - 3k_y^2)/k + \mathcal{O}(k^3). \qquad (4)$$

TABLE I: Irreducible tensor components for the point group D_{3h}. (Terms proportional to k_z are not listed as they are irrelevant for graphene.) Notation: $\{A, B\} = \frac{1}{2}(AB + BA)$.

Γ_1	$1;\ k_x^2 + k_y^2;\ \{k_x, 3k_y^2 - k_x^2\};\ k_x\mathcal{E}_x + k_y\mathcal{E}_y;$
Γ_2	$\{k_y, 3k_x^2 - k_y^2\};\ \ B_z;\ k_x\mathcal{E}_y - k_y\mathcal{E}_x$
Γ_3	$B_xk_x + B_yk_y$
Γ_4	$B_xk_y - B_yk_x;\ \mathcal{E}_z$
Γ_5	$B_x, B_y;\ B_yk_y - B_xk_x, B_xk_y + B_yk_x;\ k_y\mathcal{E}_z, -k_x\mathcal{E}_z$
Γ_6	$k_x, k_y;\ \{k_y + k_x, k_y - k_x\}, 2\{k_x, k_y\};$
	$\{k_x, k_x^2 + k_y^2\}, \{k_y, k_x^2 + k_y^2\};\ B_zk_y, -B_zk_x;$
	$\mathcal{E}_x, \mathcal{E}_y;\ k_y\mathcal{E}_y - k_x\mathcal{E}_x, k_x\mathcal{E}_y + k_y\mathcal{E}_x$

TABLE II: Symmetrized matrices for the invariant expansion of the blocks $\mathcal{H}_{\alpha\beta}$ for the point group D_{3h}.

Block	Representations	Symmetrized matrices	
$\mathcal{H}_{66}$	$\Gamma_6 \times \Gamma_6^*$	$\Gamma_1:$	$\mathbb{1}$
	$= \Gamma_1 + \Gamma_2 + \Gamma_6$	$\Gamma_2:$	σ_z
		$\Gamma_6:$	σ_x, σ_y
$\mathcal{H}_{88}$	$\Gamma_8 \times \Gamma_8^*$	$\Gamma_1:$	$\mathbb{1}$
	$= \Gamma_1 + \Gamma_2 + \Gamma_5$	$\Gamma_2:$	σ_z
		$\Gamma_5:$	$\sigma_x, -\sigma_y$
$\mathcal{H}_{99}$	$\Gamma_9 \times \Gamma_9^*$	$\Gamma_1:$	$\mathbb{1}$
	$= \Gamma_1 + \Gamma_2 + \Gamma_3 + \Gamma_4$	$\Gamma_2:$	σ_z
		$\Gamma_3:$	σ_x
		$\Gamma_4:$	σ_y
$\mathcal{H}_{89}$	$\Gamma_8 \times \Gamma_9^*$	$\Gamma_5:$	$\mathbb{1}, -i\sigma_z$
	$= \Gamma_5 + \Gamma_6$	$\Gamma_6:$	σ_x, σ_y

We find explicit expressions for the prefactors $a_{\kappa\lambda}^{66}$ by comparing Eq. (4) with the dispersion of the TB model [6]. We get $a_{10}^{66} = \epsilon_{2p}$, $a_{61}^{66} = \frac{\sqrt{3}}{2}a(t - s\epsilon_{2p})$, $a_{12}^{66} = -\frac{3}{4}sa^2(t - s\epsilon_{2p})$, and $a_{62}^{66} = \frac{1}{8}a^2(t - s\epsilon_{2p})$, where a is the lattice constant, ϵ_{2p} the on-site term, s the overlap integral, and t the transfer integral [6].

The part of $\mathcal{H}_{66}^k$ linear in $\mathbf{k}$ is formally equivalent to the Dirac Hamiltonian for massless (chiral) fermions [13]. Also, it is related via a simple unitary transformation with the Dresselhaus [14] and the Rashba [15] term in quasi-2D systems [16]. All these models give rise to a dispersion that is linear in the limit of small $\mathbf{k}$. Yet for each of these models, the transformational properties of the basis functions under the corresponding symmetry operations are qualitatively different [17]. The Dirac equation reflects the continuous symmetries of the Lorentz group [18]. In quasi-2D systems, the k-linear Dresselhaus term is intimately related with the tetrahedral symmetry of the zinc blende structure [14], whereas the Rashba term emerges from a model with axial [16] (or hexagonal [19]) symmetry. These terms refer to electron states transforming according to spinor representations of the cor-

responding crystallographic point groups, and they are nonzero only as a consequence of spin-orbit (SO) coupling [16]. In contrast, the Hamiltonian $\mathcal{H}^k_{66}$ refers to the basis functions (1). It is applicable to spinless particles or particles for which the spin degree of freedom is decoupled from the orbital motion, and the group element $\bar{E}$ does *not* play a role [20]. From a more general perspective, we see here that the symmetries of a system determine the invariant expansion (2) and the band structure $E_n(\mathbf{k})$. Yet it is, in general, not possible to follow the opposite path and infer the symmetries of a system from the Hamiltonian and the band structure $E_n(\mathbf{k})$.

Time-reversal invariance results in additional constraints for the allowed terms in the invariant expansion (2). The valleys $\mathbf{K}$ and $\mathbf{K}'$ are inequivalent points in the star $\{\mathbf{k}\}$ that characterizes the IRs of the space group for these values of $\mathbf{k}$. When we apply the general analysis in Ref. [2] to graphene, we find that the bands at $\mathbf{K}$ and $\mathbf{K}'$ belong to the case denoted "a_2" in Ref. [2], i.e., under time reversal θ the basis functions $\{\psi_i\}$ at $\mathbf{K}$ and $\mathbf{K}'$ are linearly related via a unitary matrix $\mathbf{T}$

$$\theta\,\psi_{\mathbf{K},i} = \psi^*_{\mathbf{K},i} = \sum_j T_{ji}\psi_{\mathbf{K}',j}\,. \tag{5}$$

For our basis $\{|\rho_\mp\rangle\}$ we get $\mathbf{T} = \sigma_x$ (consistent with the discussion above). Equation (5) results in the condition [2]

$$\mathbf{T}^{-1}\mathcal{H}_{\alpha\alpha}(R^{-1}\boldsymbol{\mathcal{K}})\mathbf{T} = \mathcal{H}^*_{\alpha\alpha}(f\boldsymbol{\mathcal{K}}) = \mathcal{H}^t_{\alpha\alpha}(f\boldsymbol{\mathcal{K}}) \tag{6}$$

for the diagonal blocks $\mathcal{H}_{\alpha\alpha}(\boldsymbol{\mathcal{K}})$. Here, $*$ denotes complex conjugation and t transposition, R^{-1} is an element of D_{6h} that maps $\mathbf{K}$ on $\mathbf{K}'$ (e.g., inversion), and f depends on the behavior of $\boldsymbol{\mathcal{K}}$ under time reversal. $\mathbf{k}$ and $\mathbf{B}$ are odd under time reversal so that then $f = -1$, while $\boldsymbol{\mathcal{E}}$ has $f = 1$. Then Eq. (6) implies that all terms in Eq. (3) are allowed by time-reversal invariance, yet, e.g., the third-order invariant $k_y(3k_x^2 - k_y^2)\,\sigma_z$ is forbidden.

The existence of k-linear terms in $\mathcal{H}^k_{66}$ is intimately related to the behavior of $\mathcal{H}^k_{66}$ under time reversal characterized by Eq. (6). For comparison, consider the Γ point $\mathbf{k} = 0$ of a material with point group D_{3h}, where Tables I and II are valid, too. Yet the k-linear terms in $\mathcal{H}^k_{66}$ are then forbidden because in this case the matrices $\{X^{(\kappa)}_l\}$ can be classified as even or odd under time reversal with $\{X^{(6)}_l\}$ even [2]. We remark that the above analysis based on Eqs. (5) and (6) is not compatible with a continuous $SU(2)$-like "valley isospin" degree of freedom proposed in previous work [5, 21].

It follows from Tables I and II that a field $\mathcal{E}_z$ does not affect the electrons' motion up to terms linear in k. The lowest-order invariant involving electric fields reads $a^{66}_{23}(k_x\mathcal{E}_y - k_y\mathcal{E}_x)\sigma_z$. Similarly, a linear Zeeman splitting in a field $\mathbf{B}_\parallel = (B_x, B_y, 0)$ (and independent of k) is forbidden by symmetry. Yet the allowed invariant $\mathcal{H}^{\mathrm{Z}}_{66} = a^{66}_{22}B_z\sigma_z$ implies that electrons in graphene have an orbital magnetic moment in z direction. In contrast, for neutrinos, which are almost massless Dirac fermions, the magnetic moment is proportional to their mass [22]. The spin magnetic moment of Rashba and 2D Dresselhaus electrons has both a z and an in-plane component, though generally these are different [16].

In a field $B_z > 0$ we can utilize the usual [16] ladder operators $a^\pm = l_B(k_x \pm ik_y)/\sqrt{2}$ with magnetic length $l_B = \sqrt{\hbar/|eB_z|}$ to obtain up to linear order of $\mathbf{k}$ and B_z [$\sigma_\pm \equiv \frac{1}{2}(\sigma_x \pm i\sigma_y)$]

$$\mathcal{H}^{\mathrm{L}\pm}_{66} = a^{66}_{10}\mathbb{1} + \frac{\sqrt{2}\,a^{66}_{61}}{l_{\mathrm{B}}}\left(a^+\sigma_\mp + a^-\sigma_\pm\right) \pm a^{66}_{22}\,B_z\,\sigma_z\,, \tag{7}$$

where the upper (lower) sign applies to $\mathbf{K}$ ($\mathbf{K}'$). Both $\mathcal{H}^{\mathrm{L}+}_{66}$ and $\mathcal{H}^{\mathrm{L}-}_{66}$ have the same Landau spectrum

$$E_{n\pm} = a^{66}_{10} \pm \frac{\sqrt{2}\,a^{66}_{61}}{l_{\mathrm{B}}}\sqrt{n + \left(\frac{a^{66}_{22}}{a^{66}_{61}}\right)^2\left|\frac{\hbar B_z}{2e}\right|}, \tag{8a}$$

$$E_0 = a^{66}_{10} - a^{66}_{22}\,|B_z|\,, \tag{8b}$$

with positive integers n. Finding $E_0 \neq a^{66}_{10}$ signals broken particle-hole symmetry. For $a^{66}_{22} = 0$, Eq. (8) is identical to the spectrum of 2D massless Dirac fermions in a magnetic field B_z [23]. The spectrum (8) is obtained also for the Rashba [15] and 2D Dresselhaus [16] models in the limit of an infinite effective electron mass. This result illustrates the fact that the spectrum (8) for $B_z > 0$ and $a^{66}_{22} = 0$ is determined by the dispersion (4) at $B = 0$ but does not depend on the transformational properties of the underlying basis functions (which are different for these models).

The Hamiltonian (3) is spinless. Adding a spin-1/2 degree of freedom $\{|\uparrow\rangle, |\downarrow\rangle\}$ to the basis functions of Γ_6 gives rise to spinors that transform according to the double-group IRs Γ_8 (with representative basis functions $\{|\rho_-\uparrow\rangle, |\rho_+\downarrow\rangle\}$) and Γ_9 ($\{|\rho_-\downarrow\rangle, |\rho_+\uparrow\rangle\}$) of D_{3h}. The corresponding basis matrices are also listed in Table II. Thus we obtain the 4×4 Hamiltonian

$$\mathcal{H} = \begin{pmatrix} \mathcal{H}_{88} & \mathcal{H}_{89} \\ \mathcal{H}_{98} & \mathcal{H}_{99} \end{pmatrix}, \tag{9}$$

where each block $\mathcal{H}_{\alpha\beta}$ is given by an invariant expansion of the form (2). For the diagonal blocks, Eq. (6) again applies. (The IRs Γ_8 and Γ_9 also belong to the case a_2.)

The most important consequence of SO coupling is the matrix element $\Delta = \frac{\hbar}{2m_0^2c^2}\langle x|[\nabla V \times \mathbf{p}]_z|y\rangle$, where V is the microscopic crystal potential of graphene, so that we get $a^{88}_{10} = \epsilon_{2p} + \frac{1}{2}\Delta$ and $a^{99}_{10} = \epsilon_{2p} - \frac{1}{2}\Delta$, which implies the opening of a gap Δ between the Γ_8 and Γ_9 states [24]. This gap is analogous to the gap Δ that separates the topmost valence band in semiconductors like Ge and GaAs from the spin split-off valence band [16]. Recent calculations suggest that $\Delta \approx 1$ μeV [25]. The sign of Δ cannot be infered from our analysis.

Unlike the case of inversion-asymmetric crystal structures like zinc blende and wurtzite, SO coupling in inversion symmetric graphene does not give rise to spin splitting, i.e., with spin taken into account we get a two-fold spin degeneracy for all bands throughout the Brillouin zone [2]. Accordingly, the Hamiltonian (9) preserves the two-fold spin degeneracy (for $B = \mathcal{E} = 0$). An external field $\boldsymbol{\mathcal{E}}$ breaks the inversion symmetry and Tables I and II show that, to lowest order of k, the resulting spin splitting is due to the invariants $a_{23}^{88/99}(k_x\mathcal{E}_y - k_y\mathcal{E}_x)\sigma_z$ and several off-diagonal invariants [26]. The latter are nonzero only because of SO coupling, whereas $a_{23}^{88/99} \to a_{23}^{66}$ stay finite in the limit of vanishing SO coupling. Thus we expect the diagonal invariants due to fields $\boldsymbol{\mathcal{E}}_\parallel$ to be dominant.

Finally, we want to comment on the significance of the different transformational properties characterizing the wave functions of electrons in graphene and massless Dirac fermions. Our group-theoretical analysis suggests to divide the electronic properties of these systems into two categories: (I) those that emerge from the linear dispersion (4) but that are independent of the transformational properties of the basis functions, and (II) those that do reflect these transformational properties [17]. Clearly, the experimentally verified [27] Landau spectrum (8) belongs to category (I). Similarly, *Zitterbewegung*-like effects [28], i.e., phenomena arising due to the interference between electron states from neighboring bands [29], generally belong to category (I). In contrast, the magnetic moment belongs to category (II). Weak (anti)localization reflects the behavior of electrons moving along time-reversed paths [30], which is qualitatively different for particles with integer and half-integer spins. Thus weak (anti)localization belongs also to category (II) and our analysis implies that within the framework of the spinless Hamiltonian (3) graphene shows weak localization. More generally, the formation of multi-particle multiplets belongs to category (II). Similarly, Kramers' degeneracy only holds for particle states transforming according to spinor IRs. In this context it is not important whether the symmetry group is discrete or continuous as in both cases we can distinguish ordinary and spinor IRs.

The authors appreciate stimulating discussions with A. I. Signal and D. Culcer. They are supported by the Marsden Fund Council from Government funding, administered by the Royal Society of New Zealand. Research at Argonne National Laboratory was supported by the US Department of Energy, Office of Science, Office of Basic Energy Sciences, Contract No. DE-AC02-06CH11357. U.Z. gratefully acknowledges hospitality at the Aspen Center for Physics.

[1] A. K. Geim and K. S. Novoselov, Nature Mat. **6**, 183 (2007); C. W. J. Beenakker, Rev. Mod. Phys. **80**, 1337 (2008); A. H. Castro Neto et al., arXiv:0709.1163, to appear in Rev. Mod. Phys.

[2] G. L. Bir and G. E. Pikus, *Symmetry and Strain-Induced Effects in Semiconductors* (Wiley, New York, 1974).

[3] P. R. Wallace, Phys. Rev. **71**, 622 (1947).

[4] G. W. Semenoff, Phys. Rev. Lett. **53**, 2449 (1984); D. P. DiVincenzo and E. J. Mele, Phys. Rev. B **29**, 1685 (1984); F. D. M. Haldane, Phys. Rev. Lett. **61**, 2015 (1988).

[5] E. McCann et al., Phys. Rev. Lett. **97**, 146805 (2006).

[6] R. Saito, G. Dresselhaus, and M. S. Dresselhaus, *Physical Properties of Carbon Nanotubes* (Imperial College, London, 1998).

[7] W. M. Lomer, Proc. R. Soc. Lond. A **227**, 330 (1954).

[8] G. F. Koster et al., *Properties of the Thirty-Two Point Groups* (MIT, Cambridge, MA, 1963).

[9] We define the IRs of D_{3h} via the characters listed in Table 65 of Ref. [8]. This requires that the basis functions for Γ_5 and Γ_6 of D_{3h} are reversed, see, e.g., Ref. [2].

[10] J. C. Slonczewski and P. R. Weiss, Phys. Rev. **109**, 272 (1958).

[11] H. Ajiki and T. Ando, J. Phys. Soc. Jpn. **65**, 505 (1996).

[12] Similar expressions (for $B = \mathcal{E} = 0$) were previously obtained in Refs. [4] by expanding the TB Hamiltonian around $\mathbf{K}$.

[13] J. J. Sakurai, *Advanced Quantum Mechanics* (Addison-Wesley, Reading, MA, 1967).

[14] G. Dresselhaus, Phys. Rev. **100**, 580 (1955).

[15] Y. A. Bychkov and E. I. Rashba, J. Phys. C: Solid State Phys. **17**, 6039 (1984).

[16] R. Winkler, *Spin-Orbit Coupling Effects in Two-Dimensional Electron and Hole Systems* (Springer, Berlin, 2003).

[17] For a Hamiltonian like Eq. (2) or the Dirac Hamiltonian the full wave function is the product of the solution of this Hamiltonian times the corresponding basis functions.

[18] The (restricted) homogenous Lorentz group is often denoted $SO(3,1)$. To account for spin, we need its universal covering group, which is the special linear group $SL(2)$.

[19] E. I. Rashba, Sov. Phys.–Solid State **2**, 1109 (1960).

[20] A similar situation occurs at the K points of wurtzite materials [2], yet in the absence of a center of inversion.

[21] Unlike the "valley isospin" proposed in Ref. [5], an internal spin like isospin is even under time reversal [E. C. G. Sudarshan and L. C. Biedenharn, Found. Phys. **25**, 139 (1995)]. Effective $SU(2)$ spin-1/2 models based on creation and annihilation operators for a two-level system are neither even nor odd under time reversal.

[22] K. Zuber, *Neutrino Physics* (Taylor & Francis, Bristol, 2003).

[23] J. W. McClure, Phys. Rev. **104**, 666 (1956).

[24] G. Dresselhaus and M. S. Dresselhaus, Phys. Rev. **140**, A401 (1965).

[25] H. Min et al., Phys. Rev. B **74**, 165310 (2006) and references therein.

[26] Similar expressions were previously obtained by C. L. Kane and E. J. Mele [Phys. Rev. Lett. **95**, 226801 (2005)], without specifying the underlying basis functions.

[27] K. S. Novoselov et al., Nature (London) **438**, 197 (2005); Y. Zhang et al., *ibid.* **438**, 201 (2005).

[28] R. Winkler, U. Zülicke, and J. Bolte, Phys. Rev. B **75**, 205314 (2007).

[29] D. Culcer and R. Winkler, Phys. Rev. B **78**, 235417 (2008).

[30] G. Bergmann, Phys. Rep. **107**, 1 (1984).